



**HAL**  
open science

# Cone-beam reconstruction from n-sin trajectories with transversely-truncated projections

Nicolas Gindrier, Rolf Clackdoyle, Simon Rit, Laurent Desbat

► **To cite this version:**

Nicolas Gindrier, Rolf Clackdoyle, Simon Rit, Laurent Desbat. Cone-beam reconstruction from n-sin trajectories with transversely-truncated projections. 6th International Conference on Image Formation in X-Ray Computed Tomography, Aug 2020, Regensburg, Germany. pp.46-49. hal-02928137v2

**HAL Id: hal-02928137**

**<https://hal.science/hal-02928137v2>**

Submitted on 9 Jun 2022

**HAL** is a multi-disciplinary open access archive for the deposit and dissemination of scientific research documents, whether they are published or not. The documents may come from teaching and research institutions in France or abroad, or from public or private research centers.

L'archive ouverte pluridisciplinaire **HAL**, est destinée au dépôt et à la diffusion de documents scientifiques de niveau recherche, publiés ou non, émanant des établissements d'enseignement et de recherche français ou étrangers, des laboratoires publics ou privés.

# Cone-beam reconstruction from n-sin trajectories with transversely-truncated projections

Nicolas Gindrier, Rolf Clackdoyle, Simon Rit and Laurent Desbat

**Abstract**—In cone-beam tomography, we define the n-sin source trajectory as having  $n$  periods of a sinusoid traced on an imaginary cylinder enclosing the object. A 2-sin is commonly known as a saddle, and it is known that the convex hull of a saddle is the same as the union of all of its chords. The convex hull of a closed trajectory is the Tuy region, where cone-beam reconstruction is possible if there are no truncated projections. However, with truncated projections, the method of differentiated backprojection and Hilbert inversion can be applied along a chord if the chord is visible (not truncated) in the projections. Here, we consider a particular transaxial truncation which prevents chords from always being visible, but we establish that the more powerful method of M-lines can be applied to ensure reconstruction in the reduced field-of-view. The 3-sin, on the other hand, has a Tuy region which is not filled by its chords, and we do not have any cone-beam theory to determine if reconstruction is possible with transverse reconstruction. In our preliminary numerical experiment, the 3-sin seemed to perform equally well as the 2-sin trajectory even though there were no chords passing through the slice we examined. We tentatively suggest that there might be other, yet unknown theory that explains why 3-sin reconstruction is possible with the specified transaxial truncation. We believe that these results on transverse truncation and reconstruction from 2-sin and 3-sin trajectories are new.

## I. INTRODUCTION

A cornerstone of cone-beam (CB) reconstruction theory is Tuy’s condition. For an object which is contained in some known convex region  $\Omega$ , a point  $x \in \Omega$  is said to satisfy Tuy’s condition if every plane passing through the point  $x$  intersects the source trajectory non-tangentially [1]. Given a source trajectory (always assumed to not intersect  $\Omega$ ), it was proved that stable image reconstruction could be achieved for the whole Tuy region provided that none of the cone-beam projections was truncated [1] (not just the Tuy region, but none of  $\Omega$  is allowed to be truncated). Conversely, Finch showed that all points of  $\Omega$  outside the Tuy region cannot be stably (and accurately) reconstructed (unless strong a priori information is available) [2]. Now, aside from the cases amenable to differentiated backprojection (DBP) techniques, see below, there is no current theory to systematically indicate which part of the Tuy region can be reliably reconstructed if some projections are truncated. In a restricted context, we explore this problem here. In view of Finch’s result, we are only interested in  $\Omega_0$  which is the

N. Gindrier, R. Clackdoyle and L. Desbat are with the TIMC-IMAG laboratory, CNRS UMR 5525 and Université Grenoble Alpes 38000 Grenoble, France. e-mail: nicolas.gindrier@univ-grenoble-alpes.fr

S. Rit is with Univ. Lyon, INSA-Lyon, UCB Lyon 1, UJM-Saint Etienne, CNRS, Inserm, CREATIS UMR5220, U1206, Centre Léon Bérard, F-69373, LYON, France.

This work was supported by the “Fonds unique interministériel” (FUI) and the European Union FEDER in Auvergne Rhône Alpes (3D4Carm project) and by the ANR (ROIdoré project ANR-17-CE19-0006-01).

intersection of  $\Omega$  with the Tuy region. For simplicity, we assume this (convex)  $\Omega_0$  is a cylinder with elliptical base and finite height.

Our context is a specific set of source trajectories, and a specific pattern of (transverse) truncation. The source trajectories under consideration in this work are “ $n$  periods of a sinusoid on the surface of a cylinder” (n-sin) where  $n \in \mathbb{N}, n > 1$ . A 2-sin trajectory is often called a “saddle” although the term saddle can refer to more general curves, see [3]. Nearly all the theoretical results here will apply to more general closed trajectories. For example, the convex hull of any n-sin trajectory (and more generally, of any closed trajectory) is the same as the Tuy region [2]. For the specific pattern of truncation, we consider a cylindrical reduced-field-of-view (RFOV) whose axis is parallel to the axis of the n-sin trajectory and whose radius is small enough that the RFOV does not contain all of  $\Omega_0$ . The RFOV is positioned to intersect the boundary of  $\Omega_0$ . The measured rays for each projection are exactly those that intersect the RFOV. Fig. 1 provides an example illustration of a 2-sin trajectory with a cylindrical  $\Omega_0$  and a possible RFOV.

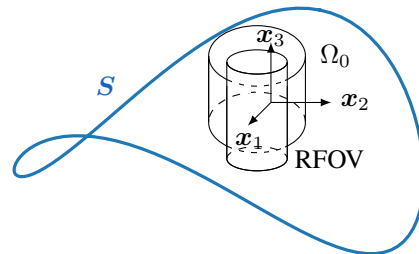


Fig. 1. A 2-sin trajectory with a cylindrical  $\Omega_0$  and a RFOV (taller than  $\Omega_0$ ).

We appeal to two methods of reconstruction when CB projections are truncated, and we refer to them here as the “DBP-chord method” and the “M-line method”. Given a source trajectory  $S$ , parametrized by  $\lambda$ , a chord  $C_{i,j}$  is a line joining  $S_{\lambda_i}$  to  $S_{\lambda_j}$  (Fig. 2 shows an example chord and an M-line). “DBP” refers to the operation or the 3D image obtained after CB backprojection of the differentiated projections. In the DBP-chord method, the DBP is performed along a sub-trajectory  $S_{[\lambda_1, \lambda_2]}$  and reconstruction takes place along the chord  $C_{1,2}$  in the DBP image, followed by an inversion of the Hilbert transform. An M-line is a half-line starting at some source point  $S_{\lambda_M}$  and passing through  $\Omega_0$ ; see Fig. 2. In the M-line method, the Hilbert inversion takes place along a segment of the M-line. The M-line method is more powerful than the DBP-chord method, but is more complicated.

In this work, we will show that the DBP-chord method is

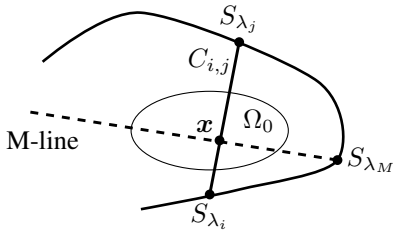


Fig. 2. A chord  $C_{i,j}$  and an M-line from  $S_{\lambda_M}$ .

not strong enough to handle the cylindrical RFOV truncation problem, but that M-line method is suitable in the case of the 2-sin trajectory. We believe this result to be new. We also demonstrate that neither the DBP-chord method nor the M-line method is suitable for certain regions inside the 3-sin trajectory. We then report on numerical experiments performed to test whether accurate reconstruction is likely to be achieved anyway, possibly due to some currently unknown theory. We point out that the simulations use an iterative reconstruction method, the goal being to test conditions for reconstruction, and not the M-line method, whose role here is purely theoretical.

Similar results on using the M-line method to verify reconstruction theory for the cylindrical RFOV have been published for the case of a helical trajectory [4]. Note the helix is not a closed trajectory, which results in different considerations than for the proof that the 2-sin trajectory admits full (accurate and stable) reconstruction throughout  $\Omega_0 \cap \text{RFOV}$ .

## II. THEORY

### A. Definitions and standard results

The unknown density function is denoted  $f(\mathbf{x})$ , where  $\mathbf{x} = (x_1, x_2, x_3)$ . For fixed height  $H$  and radius  $R$  ( $H, R > 0$ ) and for  $n \in \mathbb{N}, n > 1$  (usually  $n = 2$  or  $3$ ) we define the  $n$ -sin trajectory as

$$S_\Lambda^n = \{(R \cos \lambda, R \sin \lambda, H \cos(n\lambda))^T | \lambda \in \Lambda = [0, 2\pi)\}. \quad (1)$$

For each point  $S_\lambda$  on the source trajectory, we define the CB projection with the usual formula:

$$g(\lambda, \boldsymbol{\eta}) = \int_0^{+\infty} f(S_\lambda + l\boldsymbol{\eta}) dl, \lambda \in \Lambda. \quad (2)$$

For non-truncated projections, we would have all values of  $\boldsymbol{\eta}$  in the unit sphere, but here we only allow those  $\boldsymbol{\eta}$  such that the half-line  $L_{S_\lambda, \boldsymbol{\eta}} = \{S_\lambda + l\boldsymbol{\eta} | l \in [0, \infty)\}$  intersects the RFOV.

The operation of DBP takes a segment of the source trajectory and forms a 3D image by differentiation and weighted backprojection:

$$b_{1,2}(\mathbf{x}) = \frac{1}{\pi} \int_{\lambda_1}^{\lambda_2} \frac{1}{\|\mathbf{x} - S_\lambda\|} \left. \frac{\partial}{\partial \lambda} g(\lambda, \boldsymbol{\eta}) \right|_{\boldsymbol{\eta} = \frac{\mathbf{x} - S_\lambda}{\|\mathbf{x} - S_\lambda\|}} d\lambda. \quad (3)$$

Note that  $b_{1,2}(\mathbf{x})$  can always be calculated if  $\mathbf{x} \in \text{RFOV}$  but if  $\mathbf{x} \notin \text{RFOV}$ , then  $b_{1,2}(\mathbf{x})$  is only available in rare fortuitous geometric circumstances, such as the entire subtrajectory  $S_{[\lambda_1, \lambda_2]}$  located on the ‘‘other side’’ of the RFOV with respect to the location of  $\mathbf{x}$ .

Both the DBP-chord and M-line methods achieve image reconstruction using an intermediate Hilbert transform. For Hilbert

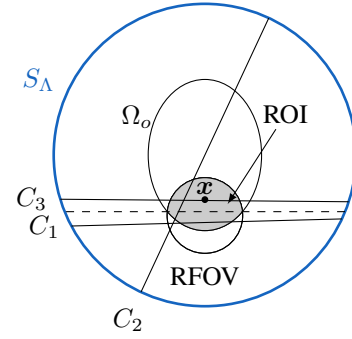


Fig. 3. Top-view for the configuration of Fig. 1. The dashed line delimits the 3 cases of reconstruction for chords containing a point in the ROI: both endpoints of  $C_1$  are below the dashed line ( $C_1$  intersects the support before the RFOV) therefore the inverse of the finite Hilbert transform can be used,  $C_2$  crosses the dashed line then the one-endpoint Hilbert transform must be used, and both endpoints of  $C_3$  are above the dashed line ( $C_3$  intersects the RFOV before the support) so there is no reconstruction from the chord method (from eq. (5)). To reconstruct  $\mathbf{x}$ , belonging to  $C_3$ , the M-line method must be used.

transforms of 3D functions, we specify a direction  $\boldsymbol{\theta}$  and use the following formula

$$\mathcal{H}_{\boldsymbol{\theta}} f(\mathbf{x}) = \int_{-\infty}^{+\infty} \frac{f(\mathbf{x} - s\boldsymbol{\theta})}{\pi s} ds \quad (4)$$

where the integral in equation (4) is in the sense of the Cauchy principal value.

### B. The DBP-chord method

The DBP-chord method is based on a link between the DBP image and the Hilbert transform. If  $\mathbf{x} \in C_{i,j}$  (and  $\mathbf{x} \in \text{RFOV}$ ), then it is well-known (e.g. [5]) that

$$b_{i,j}(\mathbf{x}) = 2\mathcal{H}_{\boldsymbol{\eta}_{i,j}} f(\mathbf{x}) \quad (5)$$

where  $\boldsymbol{\eta}_{i,j} = (S_i - S_j) / \|S_i - S_j\|$  in the direction from  $S_j$  to  $S_i$ . ‘‘One dimensional’’ image reconstruction is performed along the chord segment  $Q = C_{i,j} \cap (\Omega_0 \cup \text{RFOV})$ , provided at least one endpoint of  $Q$  lies outside  $\Omega_0$  [6]. If both endpoints lie outside  $\Omega_0$ , then an analytic formula can be used to invert  $\mathcal{H}_{\boldsymbol{\eta}_{i,j}} f$  to obtain  $f$  along  $Q$  (see [7]). If neither endpoint lies outside  $\Omega_0$ , then the DBP-chord method fails for this chord. Fig. 3 illustrates these three possibilities.

The DBP-chord method has been known for at least 15 years, and provides a powerful method for CB reconstruction with truncated projections. The only requirement to reconstruct along a chord  $C_{i,j}$  is that the chord remains visible (not truncated) in all the projections in the subtrajectory  $S_{[\lambda_i, \lambda_j]}$ , and that the field-of-view is large enough that the chord extends beyond the object boundary.

### C. The M-line method

For some  $\lambda_M$  and some direction  $\boldsymbol{\eta}_M$ , consider the M-line  $L_{S_M, \boldsymbol{\eta}_M}$  (where we have written  $S_M$  for  $S_{\lambda_M}$ ). If  $\mathbf{x} \in L_{S_M, \boldsymbol{\eta}_M}$  and  $\mathbf{x}$  also lies on a chord  $C_{1,2}$ , then

$$b_{1,M}(\mathbf{x}) + b_{2,M}(\mathbf{x}) = 2\mathcal{H}_{\boldsymbol{\eta}_M} f(\mathbf{x}). \quad (6)$$

Note that the Hilbert direction is along the M-line, and not along the chord  $C_{1,2}$ .

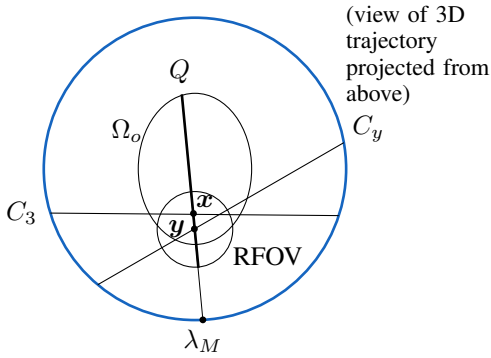


Fig. 4. The M-line method. The point  $x$  cannot be reconstructed by the DBP-chord method using its chord  $C_3$ . A suitable (one-endpoint) M-line is chosen passing through  $x$ . If each  $y \in Q \cap \text{RFOV}$  lies on some chord  $C_y$ , then the Hilbert transform can be computed, and Hilbert inversion along  $Q$  is possible, to reconstruct  $f$  at  $x$  (and at all  $y$ ).

The M-line method is designed to handle reconstruction at a point  $x$  which lies on a chord not suitable for Hilbert inversion. In that case, an M-line through  $x$  is selected which also has the property that (at least) one endpoint of  $Q$  lies outside  $\Omega_0$ , where  $Q = L_{S_M, \eta_M} \cap (\Omega_0 \cup \text{RFOV})$ . In order to invoke Hilbert inversion along  $Q$ , each point  $y \in Q \cap \text{RFOV}$  must lie on its own chord  $C_{1,2}$ , for in this case, (6) can be applied to obtain  $\mathcal{H}_{\eta_M} f(y)$ . Once  $\mathcal{H}_{\eta_M} f(y)$  has been obtained for all  $y \in Q \cap \text{RFOV}$ , then Hilbert inversion can be applied along  $Q$  to obtain  $f(x)$ . See Fig. 4 for an illustration of the concept.

The M-line method was introduced by Pack *et al.* [8], and although it is more complicated to apply, it is more powerful than the DBP-chord method due to the requirement that the Hilbert segment  $Q$  needs one endpoint outside  $\Omega_0$ .

#### D. The 2-sin trajectory

The 2-sin trajectory, equation (1), also known as a saddle, has the property that its convex hull is equal to the union of all its chords [3], see Fig. 5. Thus every point in the Tuy region lies on a chord, so if there is only moderate truncation of the projections in the axial direction, all chords will be visible in the projections, and the DBP-chord method ensures reliable reconstruction throughout the Tuy region.

For transverse truncation dictated by the cylindrical RFOV, the situation is more complex, and the three cases shown in Fig. 3 arise. Any point  $x$  inside  $\Omega_0 \cap \text{RFOV}$  will lie on a chord, which will be suitable for two-endpoint inversion ( $C_1$  in Fig. 3), for one-endpoint inversion ( $C_2$  in Fig. 3), or not suitable for Hilbert inversion ( $C_3$ ). In this latter case, it is always possible to choose an M-line joining  $x$  to the trajectory, which exits  $\Omega_0$  while still inside RFOV. All points  $y$  inside the RFOV and on this M-line will lie on some chord, from which the required Hilbert transform can be calculated according to (6). Thus Hilbert inversion is possible in all three cases, and the entire region  $\Omega_0 \cap \text{RFOV}$  can be reliably reconstructed in principle.

To the best of our knowledge, this is the first demonstration that region-of-interest reconstruction is possible with transverse truncation for the case of saddle trajectories. For a cylindrical RFOV intersecting the boundary of  $\Omega_0$ , our argument clearly

generalizes to any trajectory whose Tuy region is equal to the union of its chords. The restriction of a cylindrical RFOV can be relaxed also, but with care because combined axial and transverse truncation introduces new complications (the existence of a suitable M-line is not always ensured).

#### E. The 3-sin trajectory

Unlike the 2-sin trajectory, the Tuy region of the 3-sin trajectory contains points which do not lie on any chord. In the bottom row of Fig. 5, the convex hull (Tuy region) of the 3-sin curve consists of a triangular “roof” and triangular “floor” but there is a substantial triangular “hole” of locations which are not traversed by any chord, as shown bottom right of Fig. 5.

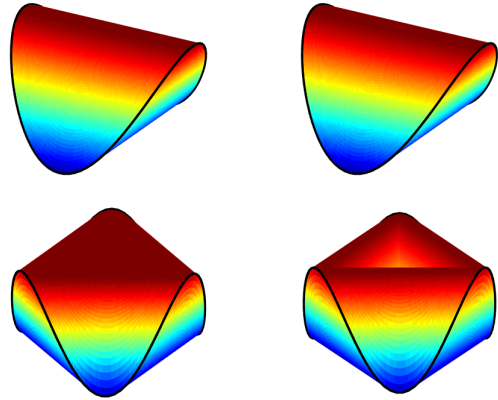


Fig. 5. The convex hull and the “chord hull” of two source trajectories. *Top*: the 2-sin trajectory. *Bottom*: the 3-sin trajectory. *Left*: the convex hull of the trajectory (the Tuy region). *Right*: the union of all chords in the trajectory.

For points in the Tuy region not lying on any chord, both the DBP-chord method and the M-line method fail, even if there were no projection truncation. However, other theory (still unknown) might indicate whether or not reconstruction is possible in regions where there are no chords. Our preliminary simulation experiments below suggest that, for cylindrical RFOV, reliable reconstruction might still be possible where chords are missing.

### III. SIMULATIONS

We performed reconstructions on a 380 x 152 x 382 image array from analytically simulated projection data of the Forbild Thorax phantom. Our goal could be an investigation of the vertebrae. The reconstruction method used was the conjugate gradient method from RTK (minimizes  $\|(Rf - p)\|_2^2 + \gamma \|\nabla f\|_2^2$  with  $R$  the forward projection operator and  $p$  the measured projections). In our case,  $\gamma = 100$ , 120 iterations were performed with 200 source positions. For both trajectories, the radius was 250 mm and the total height was 200 mm ( $H = 100$  mm). The RFOV was centered on the spinal column, with a radius of 50 mm and a height of 380 mm (the height of the phantom). It is illustrated in Fig. 6. Since the phantom diameter is 300 mm, the RFOV causes substantial transverse truncations.

Two cross-sections of different heights are presented through the reconstructed phantom ( $x_3 = 0$  mm and  $x_3 = 90$  mm), as illustrated in Fig. 7 and Fig. 8. The aim is to see the influence

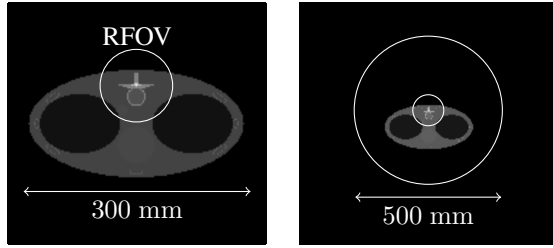


Fig. 6. Configuration in top view at  $x_3 = 0$  for simulations. *Left*: the Forbild thorax phantom and RFOV. *Right*: the trajectory with the phantom in top view.

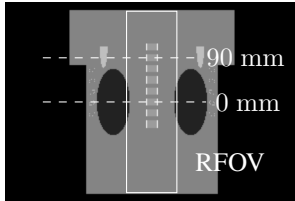


Fig. 7. Both cross-sections for the reconstruction in side view.

of the absence of chords. Specifically, for the 3-sin trajectory, the further vertically one moves away from the origin, the larger the area without chords. Results of the reconstructions are shown in Fig. 9. In the DBP theory, both cross-sections for the 2-sin trajectory can be exactly reconstructed, but for the 3-sin trajectory the cross-section  $x_3 = 90$  mm cannot be reconstructed (no chord in the RFOV, the worst case). The cross-section  $x_3 = 0$  mm is trickier: all points in the RFOV are traversed by a chord but there is no guarantee for the M-line method if it is needed (some points on the M-line must be intersected by a chord, see Section II-C above).

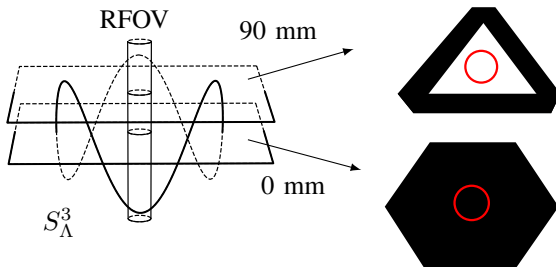


Fig. 8. *Left*: A 3-sin trajectory (not our dimensions, it is schematic) with a cylindrical RFOV and two horizontal cross-sections. *Right, above*: the set of chords (black, white means there is no chord) and the RFOV for the section  $x_3 = 90$  mm, no point in the RFOV (red circle) for this section is traversed by a chord. *Right, below*: The set of chords (black) and the RFOV for the section  $x_3 = 0$ , all points in the RFOV for this section are traversed by a chord.

We note from Fig. 9 that all four images are of good quality and comparable quality to each other in the RFOV. Since the  $x_3 = 90$  mm image for the 3-sin trajectory seemed similar to the same slice of the 2-sin trajectory, we tentatively consider that, due to some unknown reconstruction theory, this part of the Tuy region can be accurately reconstructed even though there are no chords passing through it. On the other hand, it is possible that our reconstructions are not fine enough to detect small artifacts or errors that might arise from an approximate reconstruction.

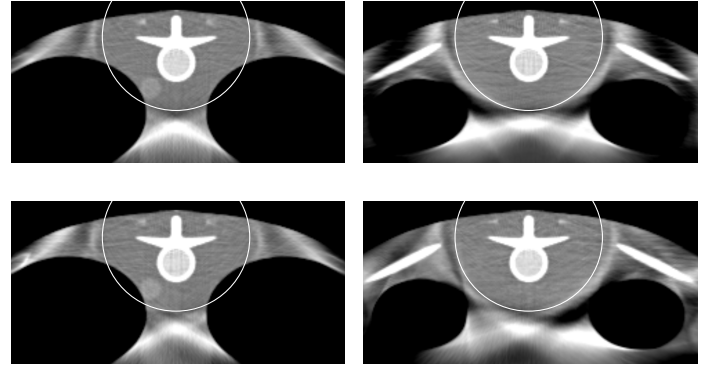


Fig. 9. Reconstruction for the 2-sin and 3-sin trajectories. *Left*:  $x_3 = 0$ . *Right*:  $x_3 = 90$  mm. *Above*:  $n = 2$ . *Below*:  $n = 3$ . White circles represent the RFOV.

#### IV. CONCLUSION

We have shown that the M-line method can be used to reconstruct an ROI with some transverse truncation, in particular for 2-sin trajectories (sinusoid on a virtual cylinder), where only axial truncations are studied in the literature. This M-lines method has some conditions, for example each point of a ROI must be intersected by a chord.

Our numerical experiments using iterative reconstructions seemed to indicate that the 3-sin trajectory with transverse truncation also produces valid reconstructions, even where there are no chords and therefore the DBP-chord and M-lines methods both do not apply.

We note also, that for any  $n > 2$ , the  $n$ -sin trajectory will have part of its Tuy region not intersected by chords. It seems likely that if reconstruction with transverse truncation is valid for 3-sin trajectories, that it will probably be valid for  $n$ -sin trajectories, for any  $n > 3$ .

There is still CB reconstruction theory to be established to resolve these questions solidly, because it appears that reconstruction can be achieved for transaxial truncation with 3-sin, at least to the extent of the sensitivity of our simulations, and the authors know of no theory to explain it.

#### REFERENCES

- [1] H. K. Tuy, "Inversion Formula For Cone-Beam Reconstruction," *SIAM Journal on Applied Mathematics*, vol. 43, no. 3, pp. 546–552, 1983.
- [2] D. V. Finch, "Cone Beam Reconstruction with Sources on a Curve," *SIAM Journal on Applied Mathematics*, vol. 45, no. 4, pp. 665–673, 1985.
- [3] J. D. Pack, F. Noo, and H. Kudo, "Investigation of saddle trajectories for cardiac CT imaging in cone-beam geometry," *Physics in Medicine and Biology*, vol. 49, no. 11, pp. 2317–2336, 2004.
- [4] R. Clackdoyle, F. Noo, F. Momey, L. Desbat, and S. Rit, "Accurate Transaxial Region-of-Interest Reconstruction in Helical CT?," *IEEE Transactions on Radiation and Plasma Medical Sciences*, vol. 1, no. 4, pp. 334–345, 2017.
- [5] R. Clackdoyle and M. Defrise, "Tomographic reconstruction in the 21st century," *IEEE Signal Processing Magazine*, no. July, pp. 60–80, 2010.
- [6] M. Defrise, F. Noo, R. Clackdoyle, and H. Kudo, "Truncated Hilbert transform and image reconstruction from limited tomographic data," *Inverse Problems*, vol. 22, no. 3, pp. 1037–1053, 2006.
- [7] F. Noo, R. Clackdoyle, and J. D. Pack, "A two-step Hilbert transform method for 2D image reconstruction," *Physics in Medicine and Biology*, vol. 49, no. 17, pp. 3903–3923, 2004.
- [8] J. D. Pack, F. Noo, and R. Clackdoyle, "Cone-beam reconstruction using the backprojection of locally filtered projections," *IEEE Transactions on Medical Imaging*, vol. 24, no. 1, pp. 70–85, 2005.